ELSEVIER

Antiviral Research 56 (2002) 189–205

Antiviral Research

www.elsevier.com/locate/antiviral

Interactions of enantiomers of 2′,3′-didehydro-2′,3′-dideoxy-fluorocytidine with wild type and M184V mutant HIV-1 reverse transcriptase

Adrian S. Ray [a], Eisuke Murakami [a], Celeste N. Peterson [a], Junxing Shi [b], Raymond F. Schinazi [b], Karen S. Anderson [a,*]

[a] *Department of Pharmacology, Yale University School of Medicine, 333 Cedar Street, New Haven, CT 06520-8066, USA*
[b] *Laboratory of Biochemical Pharmacology, Department of Pediatrics, Emory University School of Medicine/VAMC, Decatur, GA 30033, USA*

Received 18 March 2002; accepted 26 June 2002

Abstract

Both the β-D-(+) and β-L-(−)-enantiomers of 2′,3′-didehydro-2′,3′-dideoxy-5-fluorocytidine (D4FC) are clinically relevant compounds because of their potent anti-HIV and anti-HBV activities. Cross-resistance to L-D4FC with HBV containing a mutation in the conserved polymerase YMDD region has been observed. In order to better understand the effects of stereochemistry on planar 5-fluorinated cytidine analogs and to gain insight into resistance caused by YMDD mutations in HIV-1 reverse transcriptase (RT), a combination of transient kinetic studies and computer modeling were employed. In contrast to studies with the (+) and (−) isomers of 3TC-TP and FTC-TP, it was found that wild type RT had a high enantiomeric selectivity between the D-(+) and L-(−) isomers of D4FC-TP. While no resistance was conferred by the methionine 184 to valine mutation to D-D4FC-TP, L-D4FC-TP was incorporated 50- to 70-fold less efficiently. The kinetic parameters of incorporation in the presence of L-D4FC-TP by RT^{WT} and the mechanism of resistance by RT^{M184V} were found to be distinct from those seen with the corresponding L-isomers containing an oxathiolane ring: (−)-3TC-TP and (−)-FTC-TP. Molecular modeling suggests that L- and D-D4FC-TP are positioned in the active site favorably for incorporation by RT^{WT} and that L-D4FC-TP, but not D-D4FC-TP, is sterically hindered by the addition of a β branched amino acid at position 184 of RT^{M184V}.

Keywords: Antiviral agents; Transient kinetics; Nucleoside inhibitors; Molecular modeling

Abbreviations: AIDS, acquired immunodeficiency syndrome; HIV-1, human immunodeficiency virus type 1; RT, reverse transcriptase; HBV, hepatitis B virus; dNMP, deoxynucleoside 5′-monophosphate; dNTP, deoxynucleoside 5′-triphosphate; dG, 2′-deoxyguanosine; dC, 2′-deoxycytidine; dT, thymidine; D4FC, β-2′,3′-didehydro-2′,3′-dideoxy-5-fluorocytidine; 3TC, β-2′,3′-dideoxy-3′-thiacytidine; FTC, β-2′,3′-dideoxy-3′-thia-5-fluorocytidine; D4G, β-D-2′,3′-didehydro-2′,3′-deoxyguanosine; D4T, β-D-2′,3′-didehydro-3′-deoxythymidine; CBV, carbovir; NRTI, nucleoside reverse transcriptase inhibitor; RNase H, ribonuclease H; WT, wild type; M184V, methionine 184 to valine; D-D4FC is also known as REVERSET™; and (−)-FTC is known as EMTRICITABINE.

* Corresponding author. Tel.: +1-203-785-4526; fax: +1-203-785-7670
E-mail address: karen.anderson@yale.edu (K.S. Anderson).

0166-3542/02/$ - see front matter
PII: S0166-3542(02)00102-X

1. Introduction

Human immunodeficiency virus (HIV) is the causative agent of acquired immunodeficiency syndrome. HIV requires reverse transcriptase (RT) to copy its single stranded RNA genome into a double stranded DNA copy for integration into the host cell DNA. While most steps in the HIV replication cycle have been targeted (De Clercq, 1995, 1997; Mitsuya et al., 1991), a substantial number of drugs that have been effective in patient treatment are nucleoside reverse transcriptase inhibitors (NRTI's) that cause chain termination of elongating viral transcripts. Hepatitis B virus (HBV) also requires an RNA-directed DNA polymerase to copy its viral genome and chronic infection with this virus has become a worldwide problem affecting 300 million individuals (Lee, 1997). It is believed that, like HIV, the most effective anti-HBV drugs will be nucleoside inhibitors (De Clercq, 1999; Torresi and Locarnini, 2000; Furman et al., 1992). The use of nucleosides as an HBV treatment also leads to the possibility of agents that are effective against both viruses and this could be of value in co-infected individuals. Despite their historical success and their promise as new potent antiviral agents, certain nucleosides are limited by their toxicity to the host (Parker and Cheng, 1994) and their ability to select for resistant viruses (Larder, 1994). Other biological factors that effect the ability of these inhibitors to reduce viral replication are transport, metabolism, and incorporation of the drug.

Kinetic studies have lead to the hypothesis that there is a planar ribose ring intermediate during nucleotide incorporation by polymerases (Krayevsky and Watanabe, 1998). Transient kinetic experiments from our laboratory have supported this hypothesis by showing that RT incorporates planar nucleotide analogs with relatively high efficiencies. For instance with thymidine analogs, D4T-TP was found to be incorporated as efficiently by RT as the natural substrate dTTP (Vaccaro et al., 1999) and likewise with deoxyguanosine analogs, D4G-TP was also incorporated with an efficiency similar to dGTP, the corresponding natural substrate (Ray et al., 2002). Substitution of the oxygen in the ribose ring of deoxyguanosine with a methylene group and addition of a 2′,3′ unsaturation produced the carbocyclic analog carbovir triphosphate (CBV-TP) that was also found to be incorporated by RT, albeit an order of magnitude less efficiently than the natural substrate dGTP (Ray and Anderson, 2001; Ray et al., 2002). Their historical success, and these findings suggest that nucleosides that adopt planar ribose ring conformations may serve as potent new antiviral agents.

(−)-3TC is an essential component in many combination treatments for HIV (Perry and Faulds, 1997) and has also shown potent activity against HBV (Jarvis and Faulds, 1999; Lau et al., 2000). Studies have suggested that toxicity may be reduced by modifying the 5-position of the cytosine ring with a fluorine (Schinazi et al., 1992). It has also been found that the 5-fluoro derivative of (−)-3TC, [(−)-FTC] has more potent activity against HIV and HBV than its unfluorinated counterpart. Increased activity with HIV has been shown to be at least in part due to a higher incorporation efficiency during RNA-directed DNA synthesis in the presence of (−)-FTC-TP with HIV-1 RT (Feng et al., 1999). Another 5-fluorinated L-isomer with more potent activity against HIV and HBV than (−)-3TC is β-L-2′,3′-didehydro-2′,3′-dideoxy-5-fluorocytidine (L-D4FC, shown in Fig. 1) (Lin et al., 1996; Shi et al., 1999; Zoulim et al., 1996; Le Guerhier et al., 2000). Long term treatment with (−)-3TC causes the accumulation of resistant HIV with a mutation in the conserved YMDD motif of RT (Schinazi et al., 1993; Schuurman et al., 1995). Transient kinetic experiments have shown that the mutation of methionine 184 to valine (M184V) causes resistance to (−)-3TC-TP by decreasing the binding affinity (Wilson et al., 1996; Feng and Anderson, 1999b). (−)-3TC has also been shown to select for resistant HBV containing YMDD mutations (Tipples et al., 1996; Delaney et al., 2001) and these mutant viruses also show resistance to L-D4FC (Fu et al., 1999). These overlapping resistance profiles may indicate similarities between the HBV and HIV polymerase active sites.

L-D4FC's increased activity over (−)-3TC in cell culture may be due to a combination of

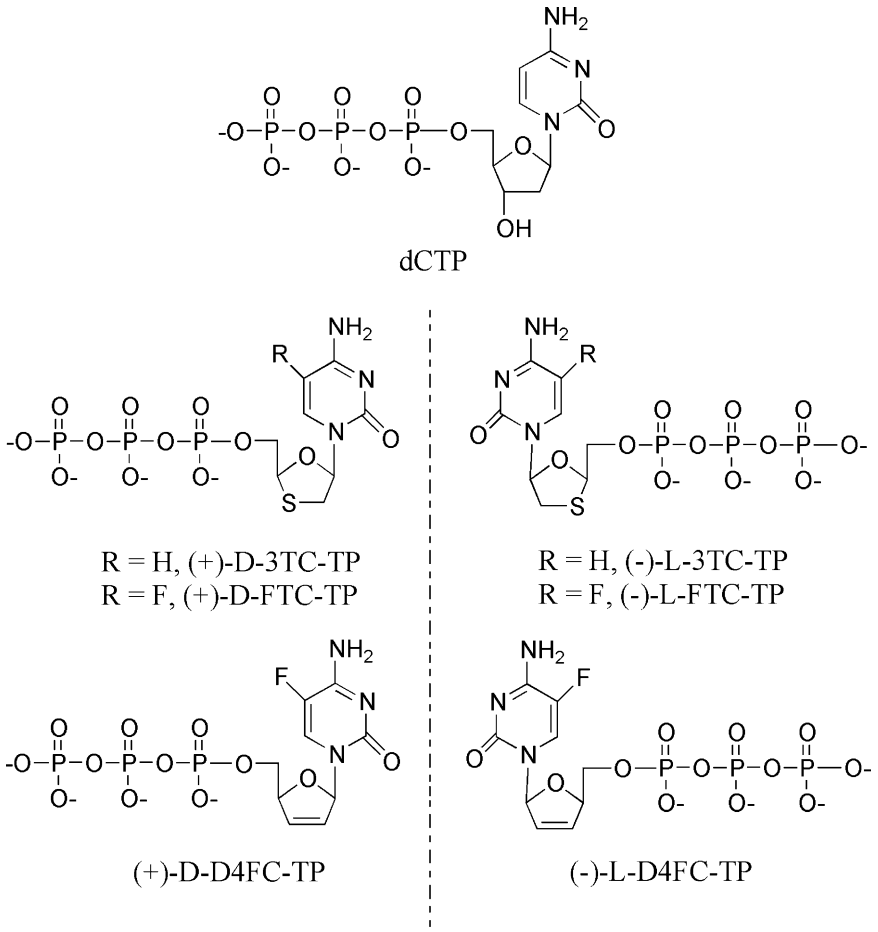

Fig. 1. Structures of enantiomeric pairs of fluorinated and unfluorinated cytidine analogs.

factors. Metabolic studies have shown that it is effectively converted to the triphosphate form and is not a substrate for cytidine deaminase (Dutschman et al., 1998). It was also found to be poorly removed by a number of cytosolic exonucleases (Pelicano et al., 2000; Kukhanova et al., 2000; Chou et al., 2000). In steady-state kinetic studies with HIV-1 RT and human polymerases, a comparison of L-D4FC-TP with (−)-3TC-TP found that it was a better substrate for HIV-1 RT as well as a good substrate for human pol γ and pol β, which might, in part, explain its toxicity (Kukhanova et al., 1998).

A steady-state kinetic analysis of L-D4FC-TP has provided a basis for understanding inhibition by this nucleoside triphosphate analog (Kukhanova et al., 1998) but is insufficient to elucidate the detailed interaction of the drug with HIV-1 RT at the polymerase active site. The reason for the limited scope of steady-state experiments is their inability to resolve kinetic steps masked by the rate-limiting step of a reaction. This point is particularly valid with the ordered reaction mechanism followed by RT (Kati et al., 1992). The first step involves binding of the DNA or RNA substrate to the enzyme to form an E·DNA complex with a dissociation constant (K_d) in the nanomolar range. This step is followed by the binding of a 2′-deoxynucleoside triphosphate (dNTP) to form the ternary complex (E·DNA·dNTP). The binding of dNTP is a two step process with an initial loose complex followed by a tighter

binding complex (Rittinger et al., 1995; Spence et al., 1995) as the enzyme undergoes the rate-limiting conformational change for catalysis (k_{pol}) and checks for correct base geometry (Kool, 1998) and proper base pairing. Once the conformational change has taken place, the 3′-hydroxyl of the elongating primer strand attacks the α phosphate of the dNTP in a rapid chemical step. The rate-limiting step for the reaction (k_{ss}) is the release of the elongated DNA from RT. This is the step analyzed during steady-state kinetic analysis and is likely not of interest in evaluating drug interactions with RT.

In order to better understand incorporation with D- and L-D4FC-TP by HIV-1 RT^{WT} and possible resistance by RT^{M184V}, a combination of transient kinetic experiments and molecular modeling were used. Molecular modeling was utilized to provide structural insight as to the possible positioning of dCTP, D-D4FC-TP, (−)-3TC-TP and L-D4FC-TP within the active site of HIV-1 RT. Data were compared with previous transient kinetic results for the (+) and (−) isomers of 3TC-TP (also commonly referred to as (+) and (−) BCH-189-TP) and FTC-TP (Feng and Anderson, 1999a,b; Feng et al., 1999).

2. Materials and methods

2.1. Purification of HIV-1 RT

RT^{WT} and RT^{M184V} were used for all experiments. The N-terminal histidine tagged heterodimeric p66/p51 enzymes were purified using clones generously provided by Dr Stephen Hughes, Dr Paul Boyer and Dr Andrea Ferris (Frederick Cancer Research and Development Center, MD). Protein purifications were performed as previously described (Kerr and Anderson, 1997b, Feng and Anderson, 1999a). Purification over cobalt affinity resin followed by anion exchange chromatography yielded protein of greater than 95% purity (as determined by protein staining of SDS-page gels, data not shown).

2.2. Nucleoside triphosphates

dCTP was purchased from Pharmacia LKB Biotechnology Inc. The preparation of D- and L-D4FC-TP was carried out as follows. To a solution of the nucleoside (D-D4FC or L-D4FC, 10 mg) in anhydrous DMF (0.3 ml) and pyridine (0.1 ml) was added a 1 M solution of 2-chloro-4H-1,3,2-benzodioxaphosphorin-4-one in anhydrous 1,4-dioxane (0.05 ml). The resulting solution was stirred at room temperature for 15 min. A solution of 1 M bis(tri-*n*-butylammonium)pyrophosphate in anhydrous DMF (0.12 ml), and Bu_3N (0.05 ml) were then added sequentially. After stirring at room temperature for another 15 min, a solution of I_2/H_2O/pyridine/THF was added to the above solution drop-wise until the iodine color persisted (about 0.5 ml). The mixture was then concentrated by evaporation in vacuo. The residue was dissolved in water (2 ml), washed with CH_2Cl_2 (3×1 ml), filtered, and purified by HPLC (column: DIONEX NucleoPac PA-100 (9×250 cm); buffer A: 0.05 M triethyl ammonium bicarbonate (TEAB); buffer B: 0.5 M triethyl ammonium bicarbonate; flow rate: 7.5 ml/min; gradient: increasing buffer B from 0% at 0 min to 50% at 10 min, 100% at 12 min, then maintained for 17 min). Collection and lyophilization of the peak with a retention time of 8–9 min afforded the product as a colorless syrup. The purity of the product, as determined by HPLC was >98% (column: DIONEX NucleoPac PA-100 (4×250); buffer A: 25 mM Tris/Cl, pH 8; buffer B: 0.5 M NaCl in 25 mM Tris/Cl, pH 8; flow rate: 1.5 ml/min; gradient: starting from 100% buffer A, by increasing buffer B from 0% at 1 min to 50% at 15 min, 80% at 18 min, then maintained for 23 min; retention time 8.9 min). MS (FAB^-) *m/e* 466 ($[M-H]^-$). Compounds were also tested for and shown to be free of contaminating pyrophosphate using the Sigma pyrophosphate kit (catalogue number P-7275) and purity was independently verified by LC-ESI mass spectrometry.

2.3. Oligonucleotides

The 18-, 23- and 45-mer DNA oligonucleotides shown in Fig. 2 were synthesized on an Applied

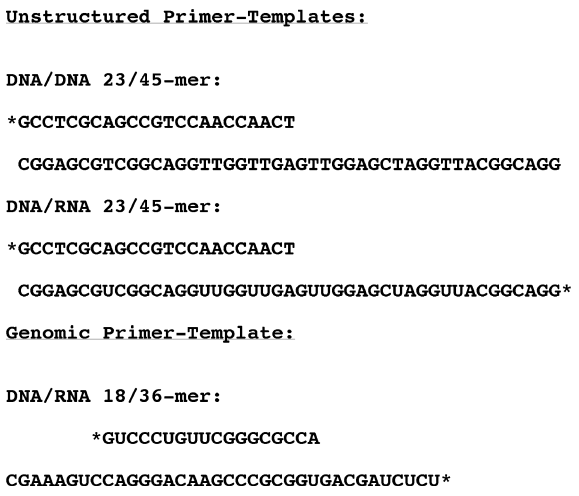

Fig. 2. Sequence of the oligonucleotide substrates. * indicates 5′-[^{32}P] labeling of the oligonucleotide.

Biosystems 380A DNA synthesizer (Keck DNA synthesis facility, Yale University) and purified using 20% polyacrylamide denaturing gel electrophoresis. The 36- and 45-mer RNA oligonucleotides were synthesized and purified by New England Biolabs.

The 18- and 23-mer DNAs and the 36- and 45-mer RNAs were 5′-^{32}P-labeled with T4 polynucleotide kinase (New England Biolabs) as previously described (Kati et al., 1992). [γ-^{32}P] ATP was purchased from Amersham/Pharmacia. Biospin columns for the removal of excess [γ-^{32}P] ATP were purchased from Bio-Rad.

Annealing of the 23- and 45-mer primer-templates (DNA/DNA and DNA/RNA), and the 18- and 36-mer primer-template (DNA/RNA) were performed by adding a 1:1.4 molar ratio of purified oligoes at 90 °C for 5 min, 50 °C for 10 min and ice for 10 min. The annealed primer-templates were then analyzed using 15% non-denaturing polyacrylamide gel electrophoresis to insure complete annealing. Concentrations of the oligonucleotides were estimated by UV absorbance at 260 nm using calculated extinction coefficients: DNA 18-mer $\varepsilon = 170{,}000\ M^{-1}\ cm^{-1}$; ; DNA 23-mer, $\varepsilon = 200{,}750\ M^{-1}\ cm^{-1}$; DNA 45-mer, $\varepsilon = 491{,}960\ M^{-1}\ cm^{-1}$; RNA 36-mer $\varepsilon = 396{,}000\ M^{-1}\ cm^{-1}$, RNA 45-mer, $\varepsilon = 507{,}960\ M^{-1}\ cm^{-1}$.

2.4. Pre-steady-state burst and single-turnover experiments

Rapid chemical quench experiments were performed as previously described with a KinTek Instruments model RQF-3 rapid-quench-flow apparatus (Kati et al., 1992; Kerr and Anderson, 1997b).

A pre-steady-state kinetic analysis was used to examine the incorporation of dCMP, D-D4FC-MP or L-D4FC-MP into a DNA/DNA or DNA/RNA duplex. No pre-steady-state burst of product formation was detected during the incorporation of L-D4FC-MP into a DNA/DNA primer-template by RT^{WT} and RT^{M184V} nor during incorporation into a DNA/RNA primer-template by RT^{M184V} indicating a change in the mechanism of incorporation and rate-limiting step. Single-turnover experiments were used under these circumstances as a means of accurate rate measurement. The reactions were carried out by rapid mixing of a solution containing the pre-incubated complex of 250 nM HIV-1 RT (wild type or M184V) and 50 nM 5′-labeled DNA/DNA duplex with a solution of 10 mM Mg^{2+} and varying the concentration of L-D4FC-TP in the presence of 50 mM Tris/Cl, 50 mM NaCl, at pH 7.8 and 37 °C (all concentrations final after mixing). Polymerization was quenched at various time points by the addition of 0.3 M EDTA. Polymerization in all other cases showed a fast phase of product formation followed by a slower steady-state phase, and pre-steady-state burst experiments were used for the analysis of polymerization. Pre-steady-state bursts were carried out under the same conditions as those described for a single-turnover experiment except the amount of primer-template (300 nM final) was in 3-fold excess of enzyme (100 nM final). DNA polymerization products were separated using 20% polyacrylamide sequencing gel analysis. Products were quantified using a Bio-Rad GS525 Molecular Imager (Bio-Rad Laboratories Inc., Hercules, CA).

2.5. Data analysis

Data were fit by non-linear regression using the program KaleidaGraph version 3.09 (Synergy

Software, Reading, PA). Results from pre-steady-state burst experiments were fit to a burst equation: $[\text{Product}] = A[1-\exp(-k_{obsd}t)+k_{ss}t]$. Where A represents the amplitude of the burst which correlates with the concentration of active enzyme, k_{obsd} is the observed first-order rate constant for dNTP or analog incorporation, and k_{ss} is the observed steady-state rate constant. Data from single-turnover experiments were fit to a single exponential equation: $[\text{Product}] = A[1-\exp(-k_{obsd}t)]$. The dissociation constant (K_d) of dCTP, D-D4FC-TP or L-D4FC-TP binding to the complex of RT and primer-template was calculated by fitting observed rate constants at different concentrations of dNTP to the following hyperbolic equation: $k_{obsd} = (k_{pol}[\text{dNTP}])/(K_d + [\text{dNTP}])$, where k_{pol} is the maximum first order rate constant for dNMP incorporation and K_d is the equilibrium dissociation constant for the interaction of dNTP with the E·DNA complex. Errors reported were calculated by standard statistical analysis (Skoog and Leary, 1992).

2.6. Molecular modeling

Computer modeling was done on a Silicon Graphics Indigo^3 Impact workstation using Insight II 95.0 software (Biosym/MSI, San Diego). All modeling was based on the crystal structure including the ternary complex of HIV-1 RT, primer-template and dTTP (Huang et al., 1998). The templating DNA base was changed from adenosine to guanosine using the biopolymer module and the replace function. A 3′ hydroxyl was modeled onto the terminal ribose ring of the primer strand, which is a dideoxy in the crystal structure. The incoming dTTP was modified to dCTP and the 3′-endo, northern ribose ring conformation found in the active sites of many DNA polymerases was conserved (for a review of nucleoside structure see Ford et al., 2000). Methionine 184 was modified to valine by using the replace function in the build module. The Val was rotated until it was in the most sterically stable position with respect to surrounding protein residues and the primer-template. The optimal positioning is similar to that found in the crystal structure of DNA bound RT^{M184I} (Sarafianos et al., 1999).

D-D4FC-TP, L-D4FC-TP and (−)-3TC-TP were built and energy minimized using the build module. Holding the ribose ring in the energy minimized planar conformation, D- and L-D4FC-TP were modeled into the active site with care being taken to have the proper base pairing and coordination of the α- and γ-triphosphate oxygens with Mg^{2+}. The planar ring conformation was found upon energy minimization and is also consistent with the crystal structure of D4T (Harte et al., 1991). (−)-3TC-TP was modeled into the active site in a S3′-exo conformation found through energy minimization and consistent with the oxathiolane ring conformation in the crystal structure of (−)-FTC (Van Roey et al., 1993). Steric interactions with Tyr 115 made it impossible to maintain proper base pairing with the templating base in the position that it is found in the crystal structure. Instead of overlapping the bases, the 3′ sulfur and 2′ carbon atoms were placed in positions to avoid steric hindrance or clashes (discussed in text). The backbone of the triphosphate was then modeled with proper coordination between Mg^{2+} and phosphate oxygens.

3. Results

In this comparative study the kinetic parameters for the addition of dCMP, D-D4FC-MP or L-D4FC-MP (triphosphate forms shown in Fig. 1) into an elongating DNA strand with either a DNA or RNA template (Fig. 2) were determined for HIV-1 RT^{WT} and RT^{M184V}. Pre-steady-state bursts and single-turnover experiments were used to define the maximum rates of incorporation (k_{pol}) and the dissociation constants (K_d) as well as to ascertain the overall rate-limiting step in the reaction pathway. These values were then used to calculate the efficiencies of incorporation (k_{pol}/K_d) to allow for comparison of D- or L-D4FC-TP with the natural substrate, dCTP. Efficiencies determined with each nucleotide with RT^{WT} and RT^{M184V} were used to calculate selectivity values for dCTP relative to the two D4FC-TP analogs (selectivity = efficiency$_{dCTP}$/efficiency$_{analog}$) to de-

termine if any resistance could be detected. Computer modeling of dCTP, (−)-3TC-TP, D-D4FC-TP and L-D4FC-TP was then used in an attempt to gain insight into kinetic phenomenon recognized in this and previous kinetic studies (Feng and Anderson, 1999a,b; Feng et al., 1999; Vaccaro et al., 1999; Ray and Anderson, 2001; Ray et al., 2002).

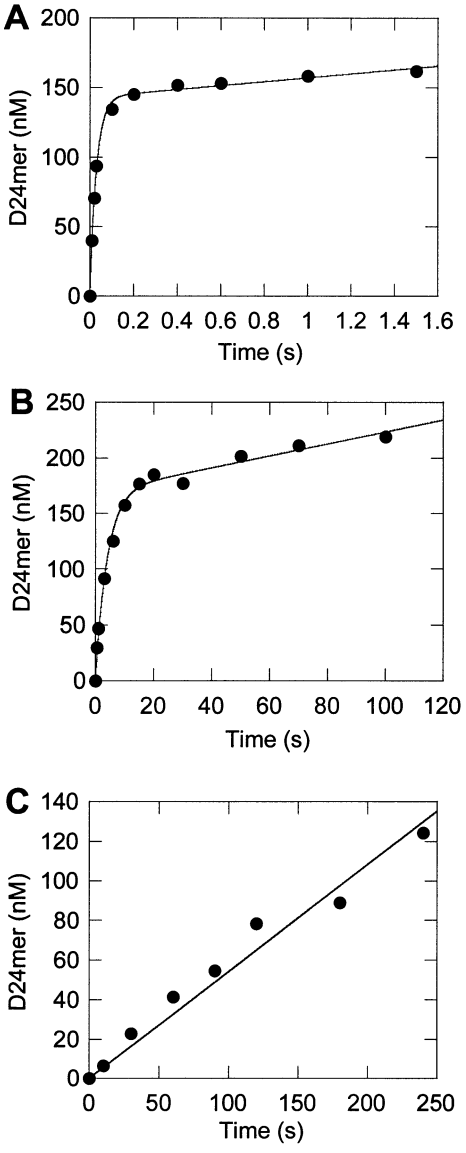

Fig. 3

3.1. Pre-steady-state incorporation with dCTP, D-D4FC-TP and L-D4FC-TP by HIV-1 RT^{WT} and RT^{M184V}

Previous studies have shown that the rate-limiting step for the catalysis of nucleotide incorporation with RT occurs after chemistry (Kati et al., 1992). When primer-template is in slight excess over enzyme this results in the observation of a burst of product, as pre-bound substrate is turned over, followed by a linear phase reflecting the rate-limiting step of product release. Previous studies with the four natural 2′-deoxynucleotides have observed bursts of product formation (Ray et al., 2002; Kati et al., 1992; Kerr and Anderson, 1997a; Feng and Anderson, 1999a). Consistent with previous results, incorporation of dCMP into both homoduplex and heteroduplex primer-templates showed a burst of product followed by a slower linear phase for both RT^{WT} and RT^{M184V} (representative dCTP curve shown in Fig. 3A).

The presence of a pre-steady-state burst during the incorporation of an analog suggests that it is being incorporated by a similar kinetic mechanism as natural dNMPs. A pre-steady-state burst of product formation was observed in all cases for D-D4FC-TP (data not shown) and a burst of product formation was observed for heteroduplex elongation with L-D4FC-TP and wild type enzyme (Fig. 3B). Elongation of a homoduplex with L-D4FC-TP by RT^{WT} and RT^{M184V} and the heteroduplex by RT^{M184V} (Fig. 3C), however, did not show a pre-steady-state burst of product indicating a change in the rate-limiting step.

Fig. 3. Change in the kinetic mechanism of polymerization for RT^{M184V} from the scheme observed with RT^{WT} during RNA-directed polymerization with L-D4FC-TP. A pre-steady-state burst experiment was done in the presence of 220 μM dCTP and a DNA/RNA primer-template which shows the typical biphasic pattern seen during incorporation in the presence of natural dNTPs and that was observed during incorporation in all cases with D-D4FC-TP (Panel A). Similar experiments were done with L-D4FC-TP with RT^{WT} (panel B) and RT^{M184V} (Panel C). RT^{WT} showed a single exponential burst of product formation followed by a slower linear phase while RT^{M184V} only shows a linear phase. The absence of a burst shows that the mechanism of incorporation has changed and that the overall rate-limiting step of the reaction occurs before or during catalysis.

3.2. Determination of the K_d and k_{pol} for incorporation with dCTP, D-D4FC-TP and L-D4FC-TP by HIV-1 RT^{WT} and RT^{M184V}

The interaction between dCTP, D-D4FC-TP and L-D4FC-TP with the E·DNA complexes were determined by plotting the observed rate (k_{obsd}) at various concentrations of nucleotide with RT^{WT} or RT^{M184V} and DNA/DNA or DNA/RNA primer-template and fitting the data to hyperbolic curves. These curves gave the maximum rate of incorporation of the dNMP (k_{pol}) and the binding affinity (expressed as the concentration of dNTP necessary to obtain the half-maximal rate) for dCTP, D-D4FC-TP, or L-D4FC-TP (K_d) with each of the E·DNA combinations.

Pre-steady-state burst experiments were used to determine the kinetic constants for dCMP incorporation by RT^{WT} and RT^{M184V} into homo- and heteroduplex primer-templates. The curve generated to fit the plot of observed rate versus dCTP concentration for RT^{WT} and a DNA/RNA primer-template gave a K_d of 48 μM and a k_{pol} of 38 s^{-1}. These values were then used to calculate the efficiency of incorporation with dCTP by RT^{WT} into a DNA/RNA primer-template to be 0.79 $\mu M^{-1}\,s^{-1}$ (data summarized in Table 1). Similar analysis showed that dCTP had a K_d of 56 μM, a k_{pol} of 2.9 s^{-1} and an efficiency of incorporation of 0.052 $\mu M^{-1}\,s^{-1}$ for a DNA/DNA primer-template. Similar analysis was done for RT^{M184V} and both primer-template combinations. In general the K_d was found to be weaker and the k_{pol} faster when comparing mutant to wild type enzyme incorporation in the presence of dCTP. Curves for RT^{WT} and RT^{M184V} and homo- and heterodulex are shown in Fig. 4A and Fig. 5A and all data are summarized in Table 1.

Results for D-D4FC-TP were similar to those seen for dCTP. Pre-steady-state bursts were done to determine the concentration dependence on rate for incorporation of a chain terminating D-D4FC-MP nucleotide during DNA- and RNA-directed synthesis by RT^{WT} and RT^{M184V}. The generated K_d curves show that the efficiencies of incorporation with D-D4FC-TP are within 3-fold of those obtained with dCTP for both enzymes and both primer-template combinations (Fig. 4B and Fig. 5B and summarized in Table 1). This data shows that RT^{M184V} has no kinetic advantage over RT^{WT} at selecting dCTP over D-D4FC-TP.

L-D4FC-TP showed no pre-steady-state burst of product formation during DNA-directed polymerization by RT^{WT}. The generated curve for RT^{WT} and a DNA/DNA primer-template (Fig. 4C) showed a k_{pol} of 0.089 s^{-1}, a K_d of 31 μM and an efficiency of incorporation of 0.0029 $\mu M^{-1}\,s^{-1}$. A burst of product formation was observed during RNA-directed polymerization. The efficiency of incorporation with L-D4FC-TP during RNA-directed polymerization by RT^{WT} was found to be an order of magnitude more efficient than during DNA-directed synthesis. This increase in efficiency was due to a marked increase in rate during RNA-directed synthesis (Fig. 5C, data summarized in Table 1). While the kinetics of incorporation of (−)-3TC-MP and (−)-FTC-MP into the DNA/RNA primer-template used in this study have been reported (Feng and Anderson, 1999a; Feng et al., 1999), we verified that our results were consistent with our earlier studies. We measured the rates of incorporation at (−)-3TC-TP concentrations close to the reported K_d value (5 μM) and at a concentration approaching saturation (25 μM) and found the obtained values to be very similar to those previously determined. For instance, at a concentration of 5 μM, a rate of 0.020 ± 0.0008 s^{-1} was observed (expected rate from previous report: 0.017 ± 0.0027 s^{-1}) and at 25 μM, a rate of 0.026 ± 0.0017 s^{-1} was observed (expected rate from previous report: 0.028 ± 0.0045 s^{-1}). A comparison of the pre-steady-state kinetics of (−)-3TC-TP, (−)-FTC-TP and L-D4FC-TP is presented in Table 2. In general, the maximum rate of polymerization in the presence of L-D4FC-TP was found to be an order of magnitude faster with a weaker affinity binding to RT when compared to the corresponding oxathiolane compounds.

While incorporation of L-D4FC-MP into an elongated DNA strand templated by RNA showed a pre-steady-state burst of product with RT^{WT} (Fig. 3B), incorporation by RT^{M184V} did not show a pre-steady-state burst of product (Fig. 3C) indicating a change in mechanism and overall rate-limiting step. The major difference in the

Table 1
Kinetic and equilibrium constants for binding and incorporation with dCTP, and D- or L-D4FC-TP by wild type and M184V HIV-1 RT

Primer/template	RT	Nucleotide	k_{pol} (s^{-1})	K_d (μM)	Efficiency ($\mu M^{-1}\ s^{-1}$)	Selectivity[a]
DNA/DNA	WT	dCTP	2.9±0.16	56±9.8	0.052±0.0095	–
		D-D4FC-TP	0.95±0.067	31±6.4	0.031±0.0068	2
		L-D4FC-TP	0.089±0.0046	31±3.5	0.0029±0.00036	20
	M184V	dCTP	6.7±0.40	68±12	0.099±0.018	–
		D-D4FC-TP	1.4±0.13	24±5.5	0.058±0.014	2
		L-D4FC-TP	0.011±0.0005	130±10	0.000085±0.000008	1000
DNA/RNA	WT	dCTP	38±2.5	48±8.3	0.79±0.14	–
		D-D4FC-TP	4.4±0.2	19±2	0.23±0.034	3
		L-D4FC-TP	0.67±0.064	27±5.3	0.025±0.0055	30
	M184V	dCTP	43±2.1	130±18	0.33±0.048	–
		D-D4FC-TP	3.2±0.20	16±3.0	0.20±0.04	2
		L-D4FC-TP	0.0068±0.0005	44±6.0	0.00016±0.000025	2000

[a] Selectivity = $\text{efficiency}_{dCTP}/\text{efficiency}_{analog}$.

interaction of the L-D4FC-TP with wild type and mutant enzyme was reflected by a two order of magnitude drop in the maximum rate of incorporation (k_{pol}) from RT^{WT} to RT^{M184V} (0.67 versus 0.0068 s^{-1} respectively, Fig. 5C) was noted. The DNA-directed polymerization kinetics showed no burst of product formation with either RT^{WT} or RT^{M184V} during DNA/DNA incorporation however a similar decrease in the maximum rate was observed in response to the M184V mutation (0.089 versus 0.011 s^{-1} respectively, Fig. 4C). These differences in rate were accompanied by only a 2- to 4-fold weakening in binding affinity (K_d). These data are consistent with RT^{M184V} being 50- and 70-fold more selective for the natural substrate, dCTP over L-D4FC-TP, than RT^{WT} during DNA- and RNA-directed polymerization respectively (summarized in Table 1). In order to insure that there was no primer-template sequence dependence upon the observed kinetics, we examined the reaction kinetics using a different oligonucleotide substrate. Accordingly, we carried out additional experiments in order to affirm that the mechanism of RT^{M184V} resistance to L-D4FC-TP is independent of primer-template and to allow for a direct comparison with (−)-3TC-TP resistance data generated with another primer-template (Feng and Anderson, 1999b). These experiments were conducted with an 18-mer DNA and a 36-mer RNA primer-template derived from the HIV genomic sequence. Consistent with data determined with the 23-mer DNA and 45-mer RNA primer-template, experiments done at saturating concentration of L-D4FC-TP showed a near two order of magnitude drop in the rate of incorporation between wild type and mutant RT (Table 3).

4. Discussion

In this paper the transient kinetics for the incorporation of dCMP, D-D4FC-MP and L-D4FC-MP into homo- and heteroduplex primer-templates catalyzed by HIV-1 RT^{WT} and RT^{M184V} have been examined. These studies have focused on assessing the effects of stereochemistry with a planar ribose ring structure on incorporation by RT^{WT} and the selectivity of RT^{M184V}. Computer modeling was then used to gain a better understanding of the incorporation of these analogs.

Transient kinetic analysis showed that there is a large difference in the efficiency of incorporation between the D- and L-isomers of D4FC-TP. In fact, RT^{WT} only favors dCTP as a substrate by 2- to 3- fold over D-D4FC-TP. This result is similar to results obtained with D4T-TP and D4G-TP in which it was found that RT^{WT} had similar efficiencies with these analogs as their corresponding natural dNTP substrates (dTTP and dGTP,

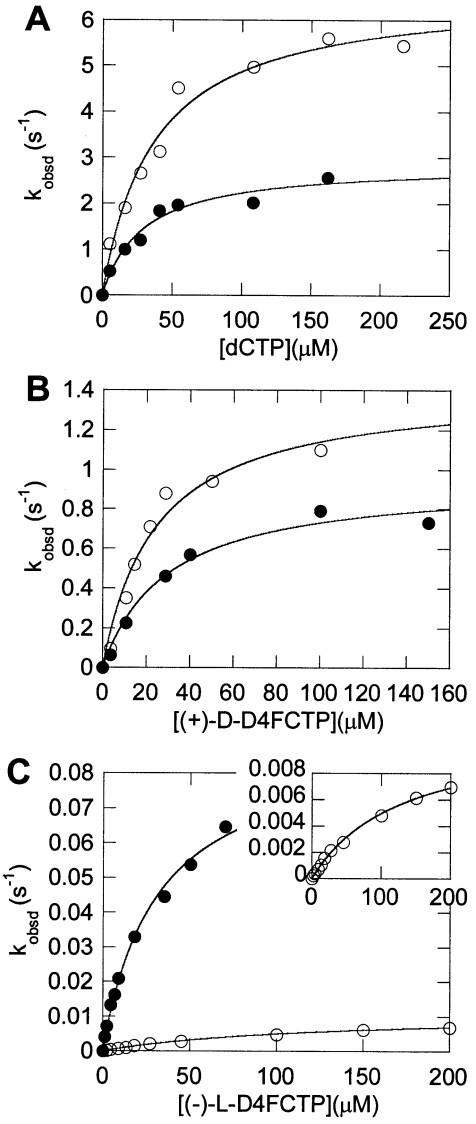

Fig. 4. Dependence of first order rate constant (k_{obsd}) on dCTP (panel A), D-D4FC-TP (panel B) and L-D4FC-TP (panel C) concentration for wild type (●) and M184V (○) RT during elongation of a DNA/DNA primer-template. The observed rate of dNMP incorporation into a DNA/DNA primer-template was plotted against the concentration of dNTP for RT^{WT} (●) and RT^{M184V} (○) and fit to hyperbolic equations. The hyperbola gave a dissociation constant for L-D4FC-TP and the primer-template bound RT (K_d) of 31 ± 3.5 μM for RT^{WT} and 130 ± 10 μM for RT^{M184V} and maximum rates of incorporation (k_{pol}) of 0.089 ± 0.0046 and 0.011 ± 0.0005 s^{-1} respectively. Inset panel C: the data for RT^{M184V} (○) was re-plotted to a more appropriate scale.

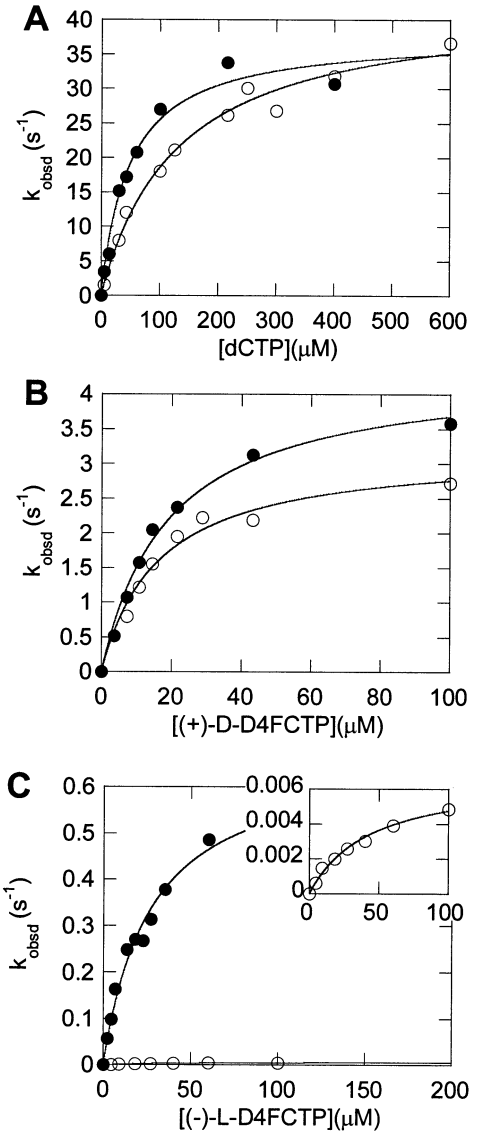

Fig. 5. Dependence of first order rate constant (k_{obsd}) on dCTP (panel A), D-D4FC-TP (panel B) and L-D4FC-TP (Panel C) concentration for wild type (●) and M184V (○) RT during elongation of a DNA/RNA primer-template. The observed rate of dNMP incorporation into a DNA/RNA primer-template was plotted against the concentrations of dNTP for RT^{WT} (●) and RT^{M184V} (○) and fit to hyperbolic equations. The hyperbola gave a dissociation constant for L-D4FC-TP and the primer-template bound RT (K_d) of 27 ± 5.3 μM for RT^{WT} and 44 ± 6 μM for RT^{M184V} and maximum rates of incorporation (k_{pol}) of 0.67 ± 0.064 and 0.068 ± 0.0005 s^{-1} respectively. Inset panel C: the data for RT^{M184V} (○) was re-plotted to a more appropriate scale.

Table 2
Both the unnatural isomers of D4FC-TP and FTC-TP are superior to (−)-3TC-TP as substrates during RNA-directed DNA polymerization by HIV-1 RT^{WT}

Analog	k_{pol} (s^{-1})	K_d (μM)	Efficiency (μM^{-1} s^{-1})
dCTP	38±2.5	48±9	0.79±0.14
(−)-L-3TC-TP[a]	0.033±0.002	5±0.8	0.0067±0.0012
(−)-L-FTC-TP[b]	0.082±0.005	1.4±0.4	0.060±0.018
(−)-L-D4FC-TP	0.67±0.064	27±5.3	0.025±0.0055

[a] Feng and Anderson (1999a).
[b] Feng et al. (1999).

Table 3
Maximum rate of incorporation of dCMP and L-D4FC-MP by HIV-1 RT^{WT} and HIV-1 RT^{M184V} into a genomic primer template

Primer/template	Nucleotide	RT	k_{Pol}[a] (s^{-1})
D18/R36(Genomic sequence)	dCTP	WT	56±5.1
		M184V	65±6.2
	(−)-L-D4FC-TP	WT	1.3±0.04
		M184V	0.017±0.0009

[a] Maximum rate of incorpotation (k_{pol}) was determined by performing an experiment at a saturating concentration of dNTP.

respectively) (Vaccaro et al., 1999; Ray et al., 2002). The low occurrence of HIV-1 RT resistance mutations to D4T (Lin et al., 1994) may be attributed to RT's inability to distinguish between D4T-TP and the natural substrate (Vaccaro et al., 1999). Similarly, D-D4FC may also have an excellent resistance profile. Lending support to this hypothesis, no resistance was conferred by the M184V mutation of RT at a kinetic level. On the other hand, L-D4FC-TP was found to be a relatively poor substrate when compared with D-D4FC-TP. Its incorporation efficiency was greater than an order of magnitude less than that of dCTP during incorporation by RT^{WT} into both hetero- and homoduplexs. It was also found that RT^{M184V} was much more sensitive to differences in stereochemistry as this mutation was shown to confer 50- and 70-fold resistance for DNA- and RNA-directed synthesis, respectively (results summarized in Table 1).

The large difference in incorporation between the D- and L-isomers of D4FC-TP is in contrast to results seen with the (+) and (−) isomers of 3TC-TP and FTC-TP where very little enantiomeric selectivity was observed on the part of RT^{WT} (Feng and Anderson, 1999a; Feng et al., 1999). The lack of enantiomeric selectivity with oxathiolane compounds may be due to the steric bulk of the sulfur atom in the ring governing the reaction kinetics and most likely does not represent a general trend for ribose ring modifications. In this study we have shown that RT does in fact have a reasonably high enantiomeric selectivity for a ribose ring alterations that cause less perturbations than elicited by the presence of sulfur in the oxathiolane ring. Moreover, these data suggest that oxathiolane compounds do not provide an exemplative model for probing L-isomers and their interactions with RT and other enzymes.

Our studies examining D- and L-D4FC-TP, were conducted with two entirely different primer-template substrates to facilitate valid comparisons with our previous work with the oxathiolane compounds (Feng and Anderson, 1999a; Feng et al., 1999). L-D4FC-MP was incorporated more efficiently than previous reported values for (−)-3TC-MP and close to the incorporation efficiency with (−)-FTC-TP during RNA-directed incorporation by RT^{WT} (Feng et al., 1999)(results summarized in Table 2). These data are consistent with cell culture findings showing that (−)-FTC and L-D4FC are more potent inhibitors of HIV than (−)-3TC (Pottage et al., 1998; Lin et al., 1996), and may suggest that the increased potency of these two compounds is due in part to higher efficiencies of incorporation by HIV-1 RT.

Many of the kinetic characteristics of incorporation in the presence of L-D4FC-TP were found to be kinetically distinct from (−)-3TC-TP and (−)-FTC-TP (results summarized in Table 2). L-D4FC-MP was incorporated approximately an order of magnitude faster than (−)-3TC-MP and (−)-FTC-MP but with a significantly weaker affinity. It is interesting that both natural and

unnatural enantiomers of analogs with planar ring structures are incorporated with relatively high rates. It is also surprising that the L-planar nucleotide binds with a weaker affinity than the oxathiolane compounds. L-D4FC-TP was found to bind with a similar affinity as dCTP to HIV-1 RT^{WT} which is consistent with results for the other planar analogs D-D4FC-TP, D4T-TP, D4G-TP and CBV-TP and there corresponding dNTPs (Vaccaro et al., 1999; Ray et al., 2002; Ray and Anderson, 2001). This is in contrast to (−)-FTC-TP and (−)-3TC-TP that bind as much as an order of magnitude more tightly at the RT^{WT} active site than dCTP depending on the primer-template combination used (Feng and Anderson, 1999a; Feng et al., 1999). One possible explanation for the tighter binding observed for (−)-FTC-TP and (−)-3TC-TP may be that there is a shift in the binding location as compared with L-D4FC-TP.

Previous clinical findings have shown that treatment of HBV with (−)-3TC causes YMDD mutations in the polymerase (Tipples et al., 1996) and these mutants of HBV are also resistant to L-D4FC (Fu et al., 1999). To see if HIV-1 RT with the M184V mutation has a similar resistance profile, we performed transient kinetic experiments with the mutant protein. It was found that RT^{M184V} was 50-fold more selective than RT^{WT} during DNA-directed polymerization (Fig. 4C) and 70-fold more selective during RNA-directed polymerization with L-D4FCTP (Fig. 5C, and summarized in Table 1). Resistance was conferred by decreases in the k_{pol} of greater than an order of magnitude and smaller changes in K_d from values obtained with RT^{WT} for both DNA/DNA and DNA/RNA primer-templates (Table 2). This is in contrast to changes in selectivity noted in a previous transient kinetic study done in our lab on (−)-3TC-TP resistance conferred by RT^{M184V}. In that study, it was found that (−)-3TC-TP resistance was caused at the level of (−)-3TC-TP binding and only slight changes in the rate of incorporation were noted (Feng and Anderson, 1999b). These resistance patterns lend further support to the hypothesis that (−)-3TC-TP binds in a way that is distinct from L-D4FC-TP in both the wild type and M184V RT active sites.

D- and L-D4FC-TP and dCTP were modeled into the active site of RT^{WT} and RT^{M184V} in order to correlate the reaction kinetics with the underlying structural consequences of modifications to the ribose ring. When modeling D- and L-D4FC-TP into the active site it was striking how well the planar ribose ring structure allowed for the cytosine base and the α phosphate to be superimposed over the corresponding positions on dCTP (Fig. 6 and Fig. 7). This optimal orientation of the base and the α phosphate may explain why analogs with 2′,3′ unsaturations and the resulting planar ring structure are incorporated so favorably by RT. For comparative purposes (−)-3TC-TP, was also modeled into the active sites of RT^{WT} and RT^{M184V} (Fig. 7). Placing (−)-3TC-TP into the active site was much more challenging than D- and L-D4FC-TP. If the cytosine ring of (−)-3TC-TP was superimposed on the base of dCTP the oxathiolane ring came into steric conflict with Tyr 115 and the α phosphate could not be positioned closer than 1 Å from the α phosphate of dCTP. Previous transient kinetic studies have shown that (−)-3TC-TP binds in such a manner as to alter the RNase H cleavage pattern and possibly the primer-template position (Feng and Anderson, 1999a). Consistent with experimental observations and our computer modeling of L-D4FC-TP, it was observed that dCTP and L-D4FC-TP had similar RNase H cleavage products while (−)-3TC-TP showed a different cleavage pattern (data not shown). Keeping these and other previously discussed kinetic differences in mind, the base was allowed to move while the oxathiolane ring 3′ sulfur and 2′ carbon were positioned in a sterically favorable position between Tyr 115, Asp 185, and Met 184 that would place the 5′ carbon in a feasible location to allowing for a reasonable positioning of the triphosphate for catalysis. The positioning of Tyr 115 may cause (−)-3TC-TP to bind in a slightly shifted binding pocket and alter the angle and positioning of the base pair to the template (Fig. 7). While this model cannot confidently predict the location of (−)-3TC-TP in the active site it clearly indicates that (−)-3TC-TP cannot occupy the same position as dTTP in the crystal structure, whereas the D4FC-TP compounds can. This could explain the slow rate of

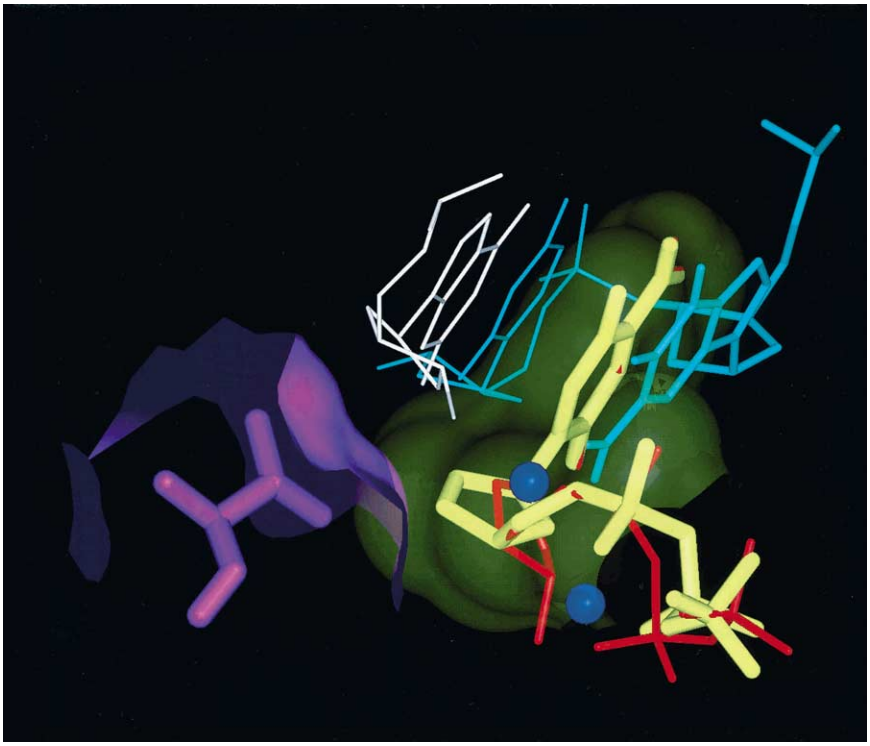

Fig. 6. Model for L-D4FC-TP (yellow) binding in the active site of the M184V mutant of HIV-1 RT. The model shows that the planar conformation of L-D4FC-TP allows for the 5-fluorocytosine base and α phosphate to be superimposed over the corresponding positions on dCTP (red). This alignment allows for L-D4FC-TP to properly base pair with the template (green), coordinate with Mg^{2+} (blue) and be aligned for attack from the 3′ hydroxyl (gray) of the 3′ terminal base of the extending primer (white). The steric clash between L-D4FC-TP and Val 184 (purple) is shown by projecting the Connolly surfaces for the two molecules.

incorporation of oxathiolane compounds and the positioning of a different template phosphodiester linkage in the distant RNase H active site and the distinct incorporation kinetics observed with (−)-3TC-TP with RT^{WT} and RT^{M184V}.

To analyze changes in dNTP binding due to the M184V mutation and a possible mechanism for resistance seen to (−)-3TC-TP and L-D4FC-TP at a structural level, we replaced Met 184 with Val. Previous modeling studies based on the crystal structure of the ternary complex (Huang et al., 1998) and different combinations of bound ligands, have shown that (−)-3TC-TP resistance may be due to steric hindrance by β branched amino acids (Val or Ile) replacing Met at position 184 (M184V or M184I) in resistant HIV-1 RT (Sarafianos et al., 1999; Gao et al., 2000). This steric clash is based on the binding of the 2′ and 3′ positions of the ribose ring of (−)-3TC-TP in the opposite orientation as natural D-dNTPs (Feng and Anderson, 1999a) and coming into close proximity to the branched side chains of M184I and M184V. Similarly, the β branched Val was found to sterically hinder (−)-3TC-TP and L-D4FC-TP by coming in close proximity to the 3′ position of the respective ring structures. This clash and the steric interaction with Tyr 115 may explain why (−)-3TC-TP resistance is observed as an exclusion from the binding pocket. The ability to fit in a sterically feasible position above Tyr 115 could explain why L-D4FC-TP resistance is characterized by a less marked reduction in binding. A repositioning of L-D4FC-TP, to avoid the contact with Val 184, may occur at the expense of optimal base pairing and/or the position of the α phosphate and as a consequence might lead to the order

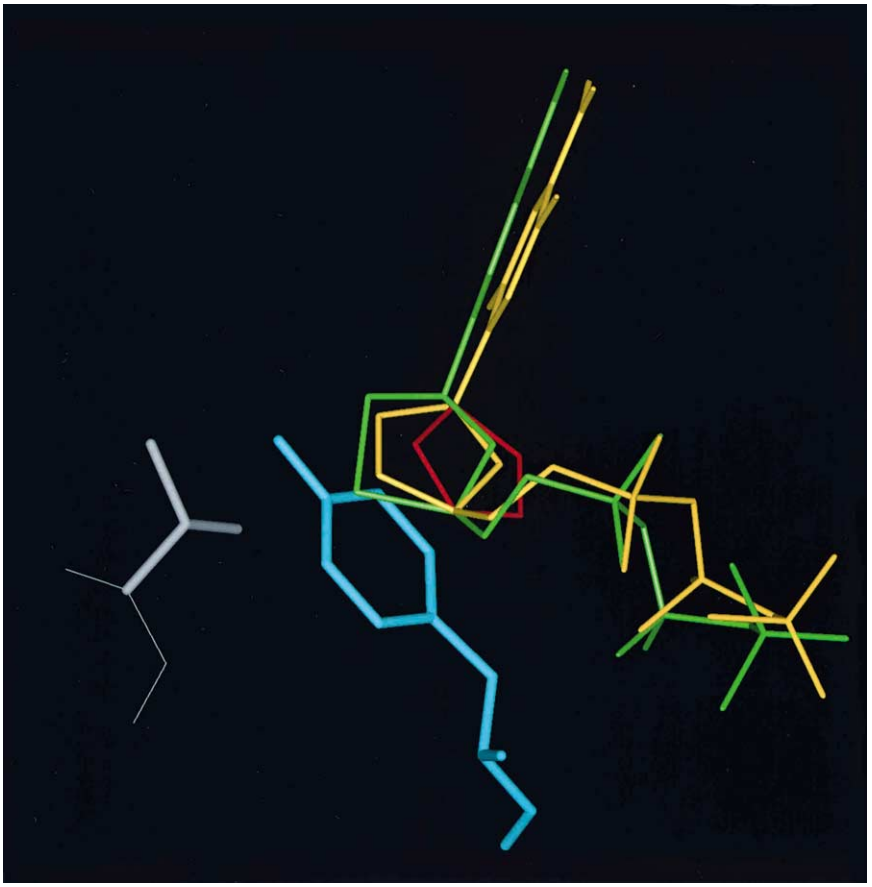

Fig. 7. Model showing the different binding positions of D-D4FC-TP (red), 3TC-TP (green) and L-D4FC-TP (yellow) in the HIV-1 RT^{M184V} active sites. In order to fit 3TC-TP into the active site without steric contact with Tyr 115 (blue) the position of the cytosine ring had to be changed. The substitution of a valine at position 184 (gray) causes a steric clash with 3TC-TP (3′ sulfur 2.41 Å from Val 184) and L-D4FC-TP (3′ Carbon 2.81 Å from Val 184) but not D-D4FC-TP (Oxygen 4.07 Å from Val 184).

of magnitude decreases in rate observed in this study.

In conclusion, we have presented a transient kinetic and computer modeling study to mechanistically describe the incorporation of D- and L-D4FC-MP by HIV-1 RT and resistance conferred by the M184V mutation of RT. From the results presented in this study, we can draw parallels to HBV polymerase, which shows similarities, in terms of substrate specificity and resistance profile, to HIV-1 RT. It was found that HIV-1 RT does have enantiomeric selectivity and suggests that oxathiolane compounds are not good general model analogs for predicting how L-nucleotides may be binding to RT. Similar to (−)-FTC-TP, L-D4FC-TP was found to be a better substrate than (−)-3TC-TP. A common theme in terms of anticipated resistance for L-nucleotides was found because, similar to (−)-3TC-TP RT^{M184V} showed high level resistance to L-D4FC-TP. D-D4FC-TP was a superior substrate and RT^{M184V} showed no advantage over RT^{WT} at selecting against D-D4FC-MP incorporation. The Tyr 115 residue may be an additional component contributing to steric hindrance to the β branched mutations occuring at position 184 and may play an important role in RT resistance to some nucleotide analogs.

Acknowledgements

We would like to thank Yung-Chi Cheng for thoughtful discussion of the data, Elias J. Fernandez for help with molecular modeling, Zhili Li and Thierry Beltran for Mass Spectrometry analysis of nucleotides, and Stephen Hughes, Paul Boyer, and Andrea Ferris for the HIV-1 RT^{WT} and HIV-1 RT^{M184V} clones. Work supported in part by NIH grants GM49551 (KSA) and R37AI-41980 (RFS), NIH National Research Service Award 5 T32 GM07223 from the National Institute of General Medical Sciences (ASR), and the Department of Veterans Affairs (RFS).

References

Chou, K.M., Kukhanova, M., Cheng, Y.C., 2000. A novel action of human apurinic/apyrimidinic endonuclease. Excision of L-configuration deoxyribonucleoside analogs from the 3′ termini of DNA. J. Biol. Chem. 275, 31009–31015.

De Clercq, E., 1995. Toward improved anti-HIV chemotherapy: therapeutic strategies for intervention with HIV infections. J. Med. Chem. 38, 2491–2517.

De Clercq, E., 1997. In search of a selective antiviral chemotherapy. Clin. Microbiol. Rev. 10, 674–693.

De Clercq, E., 1999. Perspectives for the treatment of hepatitis B virus infections. Int. J. Antimicrob. Agents 12, 81–95.

Delaney, W.E., IV, Locarnini, S., Shaw, T., 2001. Resistance of hepatitis B virus to antiviral drugs; current aspects and directions for future investigation. Antiviral Chem. Chemother. 12, 1–35.

Dutschman, G.E., Bridges, E.G., Liu, S.-H., Gullen, E., Guo, X., Kukhanova, M., Cheng, Y.-C., 1998. Metabolism of 2′,3′-dideoxy-2′,3′-didehydro-β-L(−)-5-fluorocytidine and its activity in combination with clinically approved anti-human imunodeficiency virus β−D(+) nucleoside analogs in vitro. Antimicrob. Agents Chemother. 42, 1799–1804.

Feng, J.Y., Anderson, K.S., 1999a. Mechanistic studies comparing the incorporation of (+) and (−) isomers of 3TC-TP by HIV-1 reverse transcriptase. Biochemistry 38, 55–63.

Feng, J.Y., Anderson, K.S., 1999b. Mechanistic studies examining the efficiency and fidelity of DNA synthesis by the 3TC-resistant mutant (184V) of HIV-1 reverse transcriptase. Biochemistry 38, 9440–9448.

Feng, J.Y., Shi, J., Schinazi, R.F., Anderson, K.S., 1999. Mechanistic studies show that (−)-FTC-TP is a better inhibitor of HIV-1 reverse transcriptase than 3TC-TP. FASEB J. 13, 1511–1517.

Ford, H., Dai, F., Mu, L., Siddiqui, M.A., Nicklaus, M.C., Anderson, L., Marquez, V.E., Barchi, J.J., 2000. Adenosine deaminase prefers a distinct sugar ring conformation for binding and catalysis: kinetic and structural studies. Biochemistry 39, 2581–2592.

Fu, L., Liu, S.H., Cheng, Y.C., 1999. Sensitivity of L-(−)2,3-dideoxythiacytidine resistant hepatitis B virus to other antiviral nucleoside analogues. Biochem. Pharmacol. 57, 1351–1359.

Furman, P.A., Davis, M., Liotta, D.C., Paff, M., Frick, L.W., Nelson, D.J., Dornsife, R.E., Wurster, J.A., Wilson, L.J., Fyfe, J.A., Tuttle, J.V., Miller, W.H., Condreay, L., Averett, D.R., Schinazi, R.F., Painter, G.R., 1992. The anti-hepatitis B virus activities, cytotoxicities, and anabolic profiles of the (−) and (+) enantiomers of *cis*-5-fluoro-1-[2-(hydroxymethyl)-1,3-oxathiolan-5-yl]cytosine. Antimicrob. Agents Chemother. 36, 2686–2692.

Gao, H.Q., Boyer, P.L., Sarafianos, S.G., Arnold, E., Hughes, S.H., 2000. The role of steric hindrance in 3TC resistance of human immunodeficiency virus type-1 reverse transcriptase. J. Mol. Biol. 300, 403–418.

Harte, W.E., Jr., Starrett, J.E., Jr., Martin, J.C., Mansuri, M.M., 1991. Structural studies of the anti-HIV agent 2′,3′-didehydro-2′,3′-dideoxythymidine (D4T). Biochem. Biophys. Res. Commun. 175, 298–304.

Huang, H., Verdine, G.L., Chopra, R., Harrison, S.C., 1998. Structure of a covalently trapped catalytic complex of HIV-1 reverse transcriptase: implications for nucleoside analog drug resistance. Science 282, 1669–1675.

Jarvis, B., Faulds, D., 1999. Lamivudine. A review of its therapeutic potential in chronic hepatitis B. (published erratum appears in Drugs 1999 Oct; 58 (4): 587) Drugs 58, 101–141.

Kati, W.M., Johnson, K.A., Jerva, L.F., Anderson, K.S., 1992. Mechanism and fidelity of HIV reverse transcriptase. J. Biol. Chem. 267, 25988–25997.

Kerr, S.G., Anderson, K.S., 1997a. Pre-steady-state kinetic characterization of wild type and 3′-azido-3′-deoxythymidine (AZT) resistant human immunodeficiency virus type 1 reverse transcriptase: implication of RNA directed DNA polymerization in the mechanism of AZT resistance. Biochemistry 36, 14064–14070.

Kerr, S.G., Anderson, K.S., 1997b. RNA dependent DNA replication fidelity of HIV-1 reverse transcriptase: evidence of discrimination between DNA and RNA substrates. Biochemistry 36, 14056–14063.

Kool, E.T., 1998. Replication of non-hydrogen bonded bases by DNA polymerases: a mechanism for steric matching. Biopolymers (Nucleic Acid Science) 48, 3–17.

Krayevsky, A.A., Watanabe, K.A., 1998. Substrates of DNA polymerases with planar conformation of sugar: model of substrate transition state? Nucleosides and Nucleotides 17, 1153–1162.

Kukhanova, M., Li, X., Chen, S.H., King, I., Doyle, T., Prusoff, W., Cheng, Y.C., 1998. Interaction of beta-L-2′,3′-dideoxy-2′,3′-didehydro-5-fluoro-CTP with human immunodeficiency virus-1 reverse transcriptase and human DNA polymerases: implications for human immunodeficiency virus drug design. Mol. Pharmacol. 53, 801–807.

Kukhanova, M., Liu, T.W., Pelicano, H., Cheng, Y.C., 2000. Excision of beta-L- and beta-D-nucleotide analogs from DNA by p53 protein. Nucleosides Nucleotides Nucleic Acids 19, 435–446.

Larder, B.A., 1994. Interactions between drug resistance mutations in human immunodeficiency virus type 1 reverse transcriptase. (Review) J. Gen. Virol. 75, 951–957.

Lau, D.T., Khokhar, M.F., Doo, E., Ghany, M.G., Herion, D., Park, Y., Kleiner, D.E., Schmid, P., Condreay, L.D., Gauthier, J., Kuhns, M.C., Jake Liang, T., Hoofnagle, J.H., 2000. Long-term therapy of chronic hepatitis B with lamivudine. Hepatology 32, 828–834.

Le Guerhier, F., Pichoud, C., Guerret, S., Chevallier, M., Jamard, C., Hantz, O., Li, X.Y., Chen, S.H., King, I., Trepo, C., Cheng, Y.C., Zoulim, F., 2000. Characterization of the antiviral effect of 2′,3′-dideoxy-2′,3′-didehydro-beta-L-5-fluorocytidine in the duck hepatitis B virus infection model. Antimicrob. Agents Chemother. 44, 111–122.

Lee, W.M., 1997. Hepatitis B virus infection. N. Engl. J. Med. 337, 1733–1745.

Lin, P.F., Samanta, H., Rose, R., Patick, A.K., Lee, A., Anderson, R.E., Colonno, R.J., 1994. Genotypic and phenotypic analysis of HIV-1 virus isolates from patients on prolonged stavudine therapy. J. Infect. Dis. 170, 1157–1164.

Lin, T.S., Luo, M.Z., Liu, M.C., Zhu, Y.L., Gullen, E., Dutschman, G.E., Cheng, Y.C., 1996. Design and synthesis of 2′,3′-dideoxy-2′,3′-didehydro-beta-L-cytidine (beta-L-d4C) and 2′,3′-dideoxy 2′,3′-didehydro-beta-L-5-fluorocytidine (beta-L-FD4C), two exceptionally potent inhibitors of human hepatitis B virus (HBV) and potent inhibitors of human immunodeficiency virus (HIV) in vitro. J. Med. Chem. 39, 1757–1759.

Mitsuya, H., Yarchoan, R., Kageyama, S., Broder, S., 1991. Targeted therapy of human immunodeficiency virus-related disease. FASEB J. 5, 2369–2381.

Parker, W.B., Cheng, Y.-C., 1994. Mitochondrial toxicity of antiviral nucleoside analogs. J. NIH Res. 6, 57–61.

Pelicano, H., Kukhanova, M., Cheng, Y.C., 2000. Excision of b-D- and b-L-nucleotide analogs from DNA by the human cytosolic 3(-to-5(exonuclease. Mol. Pharmacol. 57, 1051–1055.

Perry, C.M., Faulds, D., 1997. Lamivudine. A review of its antiviral activity, pharmacokinetic properties and therapeutic efficacy in the management of HIV infection. Drugs 53, 657–680.

Pottage, J., Thompson, M., Kahn, J., Delahanty, J., McCreedy, B., Rousseau, F., 1998. In: 12th World AIDS Conference in Geneva.

Ray, A.S., Anderson, K.S., 2001. Mechanistic studies to understand the inhibition of wild type and mutant HIV-1 reverse transcriptase by carbovir-triphosphate. Nucleosides Nucleotides Nucleic Acids 20, 1247–1250.

Ray, A.S., Yang, Z., Shi, J., Hobbs, A., Schinazi, R.F., Chu, C.K., Anderson, K.S., 2002. Insights into the molecular mechanism of inhibition and drug resistance for HIV-1 RT with carbovir triphosphate. Biochemistry 41, 5150–5162.

Rittinger, K., Divita, G., Goody, R.S., 1995. Human immunodeficiency virus reverse transcriptase substrate-induced conformational changes and the mechanism of inhibition by nonnucleoside inhibitors. Proc. Natl. Acad. Sci. USA 92, 8046–8049.

Sarafianos, S.G., Das, K., Clark, A.D., Jr., Ding, J., Boyer, P.L., Hughes, S.H., Arnold, E., 1999. Lamivudine (3TC) resistance in HIV-1 reverse transcriptase involves steric hindrance with beta-branched amino acids. Proc. Natl. Acad. Sci. USA 96, 10027–10032.

Schinazi, R.F., Lloyd, R.M., Jr., Nguyen, M.H., Cannon, D.L., McMillan, A., Ilksoy, N., Chu, C.K., Liotta, D.C., Bazmi, H.Z., Mellors, J.W., 1993. Characterization of human immunodeficiency viruses resistant to oxathiolane-cytosine nucleosides. Antimicrob. Agents Chemother. 37, 875–881.

Schinazi, R.F., McMillan, A., Cannon, D., Mathis, R., Lloyd, R.M., Peck, A., Sommadossi, J.-P., St. Clair, M., Wilson, J., Furman, P.A., Painter, G., Choi, W.-B., Liotta, D.C., 1992. Selective inhibition of human immunodeficiency viruses by racemates and enantiomers of cis-5-fluoro-1-[2-(hydroxymethyl)-1,3-oxathiolan-5-yl]cytosine. Antimicrob. Agents Chemother. 36, 2423–2431.

Schuurman, R., Nijhuis, M., van Leeuwen, R., Schipper, P., Collis, P., Danner, S.A., Mulder, J., Loveday, C., Christopherson, C., Kwok, S., Sninsky, J., Boucher, C.A.B., 1995. Rapid changes in human immunodeficiency virus type 1 RNA load and appearence of drug-resistant virus populations in persons treated with lamivudine (3TC). J. Infect. Dis. 171, 1411–1419.

Shi, J., McAtee, J.J., Schlueter Wirtz, S., Tharnish, P., Juodawlkis, A., Liotta, D.C., Schinazi, R.F., 1999. Synthesis and biological evaluation of 2′,3′-didehydro-2′,3′-dideoxy-5-fluorocytidine (D4FC) analogues: discovery of carbocyclic nucleoside triphosphates with potent inhibitory activity against HIV-1 reverse transcriptase. J. Med. Chem. 42, 859–867.

Skoog, D.A., Leary, J.J., 1992. Principles of Instrumental Analysis. Saunders College Publishing, New York.

Spence, R.A., Kati, W.M., Anderson, K.S., Johnson, K.A., 1995. Mechanism of inhibition of HIV-1 reverse transcriptase by nonnucleoside inhibitors. Science 267, 989–993.

Tipples, G.A., Ma, M.M., Fischer, K.P., Bain, V.G., Kneteman, N.M., Tyrrell, D.L., 1996. Mutation in HBV RNA-dependent DNA polymerase confers resistance to lamivudine in vivo. Hepatology 24, 714–717.

Torresi, J., Locarnini, S., 2000. Antiviral chemotherapy for the treatment of hepatitis B virus infections. Gastroenterology 118, S83–S103.

Vaccaro, J.A., Parnell, K.M., Terezakis, S.A., Anderson, K.S., 1999. Mechanism of inhibition of human immunodeficiency virus type 1 reverse transcriptase by d4TTP: an equivalent incorporation efficiency relative to the natrual substrate dTTP. Antimicrob. Agents Chemother. 44, 217–221.

Van Roey, P., Pangborn, W.A., Schinazi, R.F., Painter, G., Liotta, D.C., 1993. Absolute configuration of the antiviral agent (−)-*cis*-5-fluoro-1-[2-hydroxymethyl)-1,3-oxanthiolan-5-yl]cytosine. Antiviral Chem. Chemother. 4, 369–375.

Wilson, J.E., Aulabaugh, A., Caligan, B., McPherson, S., Wakefield, J.K., Jablonski, S., Morrow, C.D., Reardon, J.E., Furman, P.A., 1996. Human immunodeficiency virus type-1 reverse transcriptase. Contribution of Met-184 to binding of nucleoside 5′-triphosphate. J. Biol. Chem. 271, 13656–13662.

Zoulim, F., Dannaoui, E., Borel, C., Hantz, O., Lin, T.S., Liu, S.H., Trepo, C., Cheng, Y.C., 1996. 2′,3′-dideoxy-beta-L-5-fluorocytidine inhibits duck hepatitis B virus reverse transcription and suppresses viral DNA synthesis in hepatocytes, both in vitro and in vivo. Antimicrob. Agents Chemother. 40, 448–453.